THEORETICAL BACKGROUND

2

In this chapter the background information related to the techniques used in this PhD work is presented. The overview of the DFT-method is skipped here for which the reader is recommended to consult the comprehensive and competent works available in the literature, e.g. [27, 28]. The issues considered here are the Poisson-Boltzmann equation, continuum electrostatics, atomic partial charges, reference electrodes and spin states of transition metal complexes. In writing of this chapter I was basically guided by materials published in the following literature [29-41].

2.1 Electrostatic computations

In this part (2.1) the background is given, which is needed to understand the methods used in this PhD work for the electrostatic computations.

2.1.1 Poisson-Boltzmann equation

2.1.1.1 Derivation

Let us consider a system of point charges in a homogeneous continuum dielectric ε. In the simple case of a one charge q_1 the electrostatic potential at position P (Figure 1), is given by:

$$\phi(\mathbf{r}) = \frac{1}{4\pi\varepsilon_0\varepsilon}\frac{q_1}{|\mathbf{r}-\mathbf{r}_1|}, \tag{2.1}$$

where $\mathbf{r}$ and $\mathbf{r_1}$ are the vectors corresponding to positions of point P and charge q_1, respectively. From now on the expressions will be given in atomic units, where the factor $4\pi\varepsilon_0$ is unity. For the set of N point charges q_i the equation (2.1) generalizes to

$$\phi(\mathbf{r}) = \sum_{i=1}^{N}\frac{q_i}{\varepsilon|\mathbf{r}-\mathbf{r}_i|}. \tag{2.2}$$

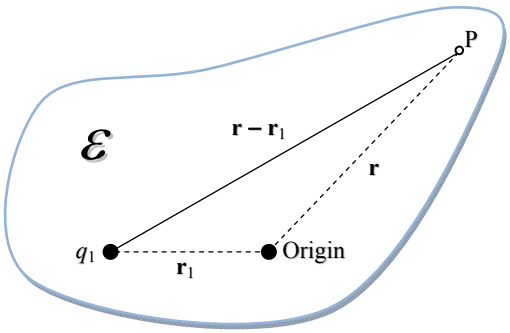

Figure 1. Simple model consisting of one charge placed in homogeneous dielectric continuum ε.

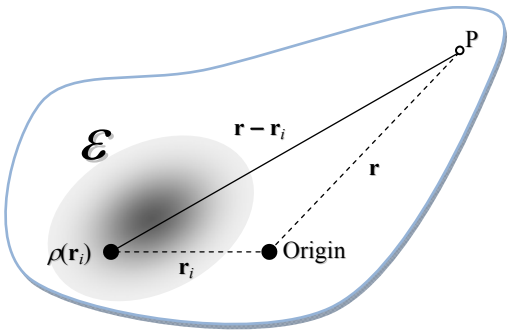

Figure 2. Electrostatic potential due to charge distribution in homogeneous dielectric continuum ε.

If dealing with the charge distributions instead of point charges (Figure 2), the electrostatic potential is defined using charge density ρ

$$\phi(\mathbf{r}) = \int_{\mathrm{V}}\frac{\rho(\mathbf{r}_i)\mathrm{d}^3\mathbf{r}_i}{\varepsilon|\mathbf{r}-\mathbf{r}_i|}. \tag{2.3}$$

Recalling that the Green's function for the three-dimensional Laplacian ∇^2 is given by $(-4\pi|\mathbf{r}-\mathbf{r}_i|)^{-1}$, and applying the Laplacian to both sides of the equation (2.2) one gets another fundamental equation of electrostatics – the Poisson equation

$$\nabla^2\phi(\mathbf{r}) = \sum_{i=1}^{N} -\frac{4\pi q_i}{\varepsilon}\delta(\mathbf{r}-\mathbf{r}_i), \tag{2.4}$$

where $\delta(\mathbf{r})$ is the Dirac delta function. Combination of equation (2.4) with expression (2.5)

$$\rho(\mathbf{r}) = \sum_{i=1}^{N} q_i\delta(\mathbf{r}-\mathbf{r}_i), \tag{2.5}$$

leads to more convenient form of Poisson equation

$$\nabla^2\phi(\mathbf{r}) = -\frac{4\pi\rho(\mathbf{r})}{\varepsilon}. \tag{2.6}$$

In the inhomogeneous medium the dielectric constant becomes dependent on the special position (Figure 3). For such cases the Poisson equation (Eq. (2.6)) adopts the more general form

$$\nabla\cdot\left[\varepsilon(\mathbf{r})\nabla\phi(\mathbf{r})\right] = -4\pi\rho(\mathbf{r}). \tag{2.7}$$

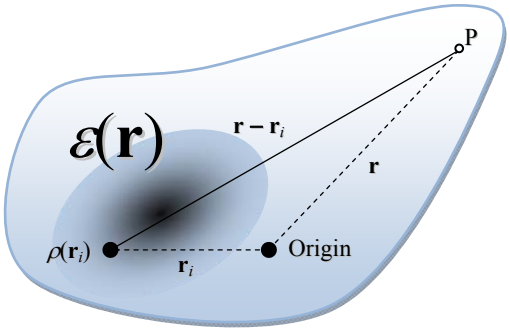

Figure 3. Electrostatic potential due to charge distribution in inhomogeneous dielectric continuum $\varepsilon(\mathbf{r})$.

Let us consider now the more complex electrostatic model containing three regions. Two- and three-dimensional views of such model are represented on the Figure 4 and Figure 5. The internal region **A** with the dielectric constant of ε_A consists of the immobile point charges and is assumed to represent the molecule for which the electrostatic potential should be determined. The external region **C** represents the solvent as a dielectric continuum with dielectric constant ε_C and may contain mobile ions [for the simplicity the electrolyte consisting of monovalen ions (from now on denotet in text as 1:1 electrolyte) is considered to be a source of the mobile ions in the region **C**]. The region **B** is a layer around the region **A**, called "ion-exclusion layer", which is penetrated by the solvent, remains however inaccessible for mobile ions. So the region **B** has the same dielectric constant ε_C as a region **C**. The thickness of the layer corresponds to the radius of the solvated ions. This system represents an extension to the basic Debye-Hückel model[42], where region **A** is just a single ion of the solution.

The electrostatic potential ϕ_A in the **A** is described by Poisson equation (Eq. (2.6)) with the charge density $\rho_A(\mathbf{r})$ and dielectric constant ε_A. Since there are no charges in the region **B**, the charge density function there is given by $\rho_B(\mathbf{r}) = 0$, leading to

$$\nabla^2\phi_B(\mathbf{r}) = -\frac{4\pi\rho_B(\mathbf{r})}{\varepsilon_C} = 0\,. \tag{2.8}$$

The electrostatic potential ϕ_C in the region **C** is determined by the charge density function of the mobile ions and dielectric constant ε_C of the solvent. Debye-Hückel theory assumes, that the mobile ions in solution are distributed according to the Boltzmann distribution law, so that the ratio of the concentration of the ions of type *s* near the molecule in A (c_s^{r}) to its concentration far away from A (c_s) is given by

$$\frac{c_s^{\mathrm{r}}}{c_s} = e^{-\frac{\mathrm{W}_i(\mathbf{r})}{kT}}, \tag{2.9}$$

where $\mathrm{W}_i(\mathbf{r})$ is the work required to move the ion of type *i* from $|\mathbf{r}| = \infty$ ($\phi(\mathbf{r}) = 0$) to the point **r**, k – Boltzmann constant and T – absolute temperature.

Since the solution in the studied model is considered to be 1:1 electrolyte solution, consisting of ions with charges $+q_s$ and $-q_s$, then

$$\mathrm{W}_+(\mathbf{r}) = +q_s\phi_C(\mathbf{r}), \quad \mathrm{W}_-(\mathbf{r}) = -q_s\phi_C(\mathbf{r}) \tag{2.10}$$

for the positive and negative ions, respectively. If c_+^{r} and c_-^{r} are the concentrations of positive and negative ions, respectively, then using Boltzmann distribution one can write

$$c_+^{\mathrm{r}} = c_s e^{-\frac{q_s\phi_C(\mathbf{r})}{kT}}, \quad c_-^{\mathrm{r}} = c_s e^{+\frac{q_s\phi_C(\mathbf{r})}{kT}}, \tag{2.11}$$

where c_s is the concentration of ions at infinite distance from **A** where the electrostatic potential vanishes ($\phi(\mathbf{r}) = 0$).

The charge density at the point **r** in the region **C** can then be determined by

$$\rho_C(\mathbf{r}) = c_+^{\mathrm{r}}q_s - c_-^{\mathrm{r}}q_s = c_s q_s e^{-\frac{q_s\phi_C(\mathbf{r})}{kT}} - c_s q_s e^{\frac{q_s\phi_C(\mathbf{r})}{kT}} = -2c_s q_s \sinh\left(\frac{q_s\phi_C(\mathbf{r})}{kT}\right). \tag{2.12}$$

For the general case equation (2.12) can be rewritten as

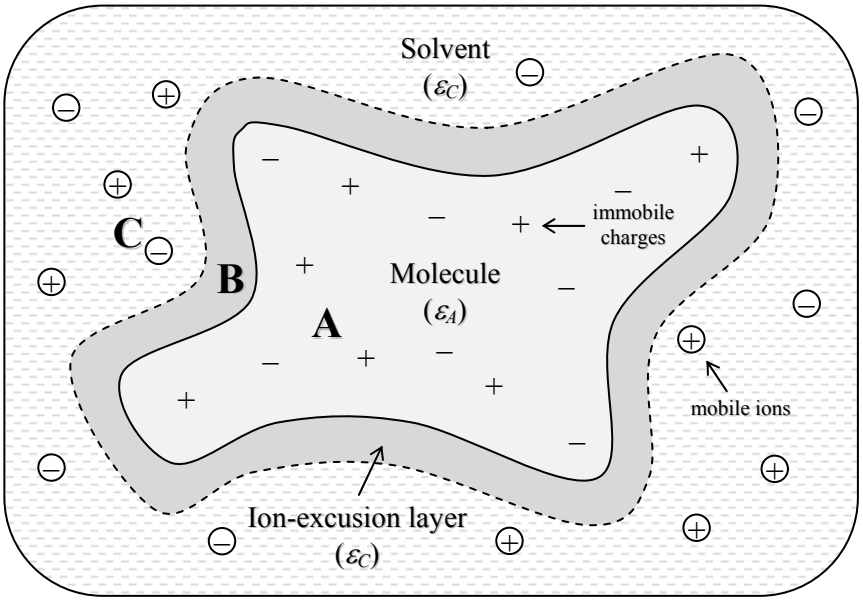

Figure 4. Schematic two-dimensional representation of the extended Debye-Hückel model, consisting of three regions (**A**, **B** and **C**). ε_A and ε_C are the dielectric constants for the appropriate regions.

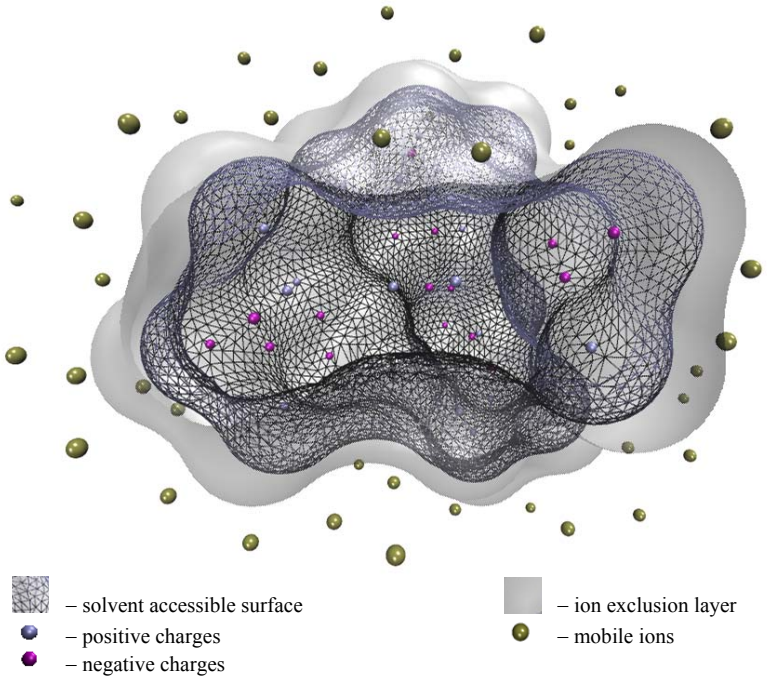

Figure 5. Three-dimensional representation of the extended Debye-Hückel model. The volume covered with meshed surface represents a region **A**, including immobile point charges. The ion-exclusion layer (**B**) surrounding region **A** is the volume between meshed and transparent-gray surfaces. The outside volume is region **C** with mobile ions.

$$\rho_C(\mathbf{r}) = \sum_{s=1}^{N_s} c_s q_s e^{-\frac{q_s \phi_C(\mathbf{r})}{kT}}, \tag{2.13}$$

where N_s is the number of different types of ions s. Accordingly, the electrostatic potential in region **C** is given by

$$\nabla^2 \phi_C(\mathbf{r}) = -\frac{4\pi\rho_C(\mathbf{r})}{\varepsilon_C} = -\frac{4\pi}{\varepsilon_C}\sum_{s=1}^{N_s} c_s q_s e^{-\frac{q_s \phi_C(\mathbf{r})}{kT}}, \tag{2.14}$$

or in our case of a 1:1 electrolyte as

$$\nabla^2 \phi_C(\mathbf{r}) = -\frac{4\pi\rho_C(\mathbf{r})}{\varepsilon_C} = \left(\frac{8\pi c_s q_s}{\varepsilon_C}\right)\sinh\left(\frac{q_s \phi_C(\mathbf{r})}{kT}\right). \tag{2.15}$$

Adding the ionic charge density [Eq. (2.13)] to the general Poisson equation [Eq. (2.7)] leads to the nonlinear Poisson-Boltzmann equation, governing the electrostatic potential $\phi(\mathbf{r})$ in all three described regions (**A**, **B** and **C**)

$$\nabla \cdot \left[\varepsilon(\mathbf{r})\nabla\phi(\mathbf{r})\right] + 4\pi\sum_{s=1}^{N_s} c_s(\mathbf{r}) q_s e^{-\frac{q_s \phi(\mathbf{r})}{kT}} = -4\pi\rho(\mathbf{r}). \tag{2.16}$$

Concentration c_s in equation (2.16) depends on the position (**r**), so that $c_s = 0$, for the $\mathbf{r} \in \mathbf{A}$ or **B**. Being nonlinear, this differential equation is difficult to solve. However it can be linearized by expanding the exponential term under the assumption that the $\frac{q_s \phi(\mathbf{r})}{kT}$ is small

$$\sum_{s=1}^{N_s} c_s(\mathbf{r}) q_s e^{-\frac{q_s \phi(\mathbf{r})}{kT}} \approx \sum_{s=1}^{N_s} c_s(\mathbf{r}) q_s - \frac{1}{kT}\sum_{s=1}^{N_s} c_s(\mathbf{r}) q_s^2 \phi(\mathbf{r}). \tag{2.17}$$

Since in the Debye-Hückel model the number of positive and negative ions is required to be the same, providing overall electroneutrality, the first summation in equation (2.17) vanishes

$$\sum_{s=1}^{N_s} c_s(\mathbf{r}) q_s = 0. \tag{2.18}$$

The second summation in equation (2.17) can be rewritten elegantly using the definition of the ionic strength (I) which is

$$I(\mathbf{r}) = \frac{1}{2}\sum_{s=1}^{N_s} c_s(\mathbf{r}) q_s^2 \,. \tag{2.19}$$

Then the Poisson-Boltzmann obtains its final linearized form

$$\nabla \cdot \left[\varepsilon(\mathbf{r})\nabla\phi(\mathbf{r})\right] - \frac{8\pi}{kT} I(\mathbf{r})\phi(\mathbf{r}) = -4\pi\rho(\mathbf{r}) \,. \tag{2.20}$$

The Debye-Hückel parameter (also called Debye screening constant) (k_D) is defined as

$$k_D^2 = \frac{4\pi}{\varepsilon kT}\sum_{s=1}^{N_s} c_s q_s^2 = \frac{8\pi I}{\varepsilon kT} = \frac{1}{l_D^2} \,, \tag{2.21}$$

where l_D is called the Debye length. The modified Debye-Hückel parameter $\bar{k}$ is given by

$$\bar{k} = k_D\sqrt{\varepsilon} \,. \tag{2.22}$$

Finally, the equation (2.20) can be rewritten using the modified Debye-Hückel parameter $\bar{k}$

$$\nabla \cdot \left[\varepsilon(\mathbf{r})\nabla\phi(\mathbf{r})\right] - \bar{k}^2(\mathbf{r})\phi(\mathbf{r}) = -4\pi\rho(\mathbf{r}) \,. \tag{2.23}$$

2.1.1.2 Numerical solution of the Poisson-Boltzmann equation

While analytical solutions of the Poisson-Boltzmann equation are available only for few idealized geometries (e.g. spherical or cylindrical), the complex geometries and charge distributions formed by most solutes, require numerical solutions. Most of the available programs use different versions of the finite difference method[43-45], where all relevant physical quantities (molecular charges, electrostatic potentials, dielectric constant and ionic strength) are discretized (mapped) on a grid, replacing differential operators by grid value differences. More recently Holst et al.[46, 47] proposed and implemented new multigrid techniques, in order to achieve faster and more accurate solutions. Among the other proposed approaches are so called boundary element method[48-50] and the finite element method[51, 52]. The program suite MEAD[53, 54] which is used in this doctoral work is solving the Poisson-Boltzmann equation using the finite difference method. The mapping is usually carried out on a cubic grid with grid constant h, by linear interpolation (Figure 6).

Integrating equation (2.23) over volume (Figure 6) yields

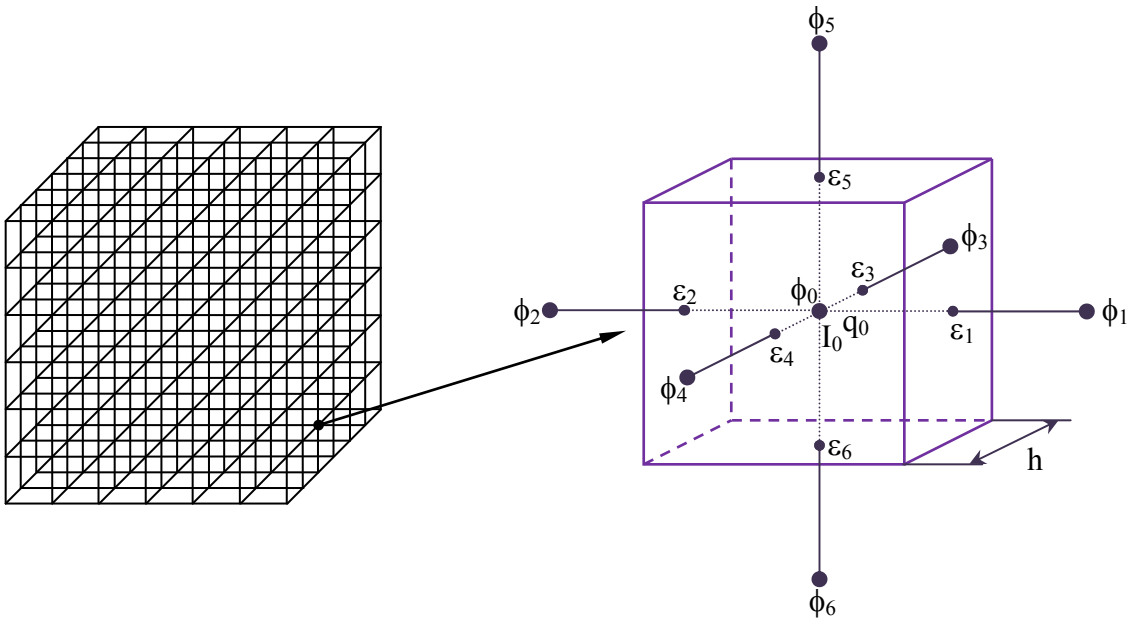

Figure 6. Three-dimensional grid and a cubic volume element related to the grid points. The dielectric constant (ε) is associated with the midpoint of the line joining neighbor grid points. The potential (ϕ), charge (q), and ionic strength (I) are associated with the center of the cube.

$$\iiint \nabla \cdot [\varepsilon(\mathbf{r})\nabla\phi(\mathbf{r})]\mathrm{d}^3\mathbf{r} - \iiint \bar{k}^2(\mathbf{r})\phi(\mathbf{r})\mathrm{d}^3\mathbf{r} = -\iiint 4\pi\rho(\mathbf{r})\mathrm{d}^3\mathbf{r}\,. \qquad (2.24)$$

The second term in equation (2.24) can be approximated by $\bar{k}_0^2\phi_0 h^3$, where $\bar{k}_0$ and ϕ_0 are respectively, modified Debye-Hückel parameter and electrostatic potential, associated with the grid point. The third integral gives $4\pi q_0$, where q is a total charge inside the volume element. The first integral can be transformed to a surface integral using Gauss's theorem

$$\iint \varepsilon(\mathbf{r})\nabla\phi(\mathbf{r})\cdot\mathrm{d}\mathbf{A} - \bar{k}_0^2\phi_0 h^3 = -4\pi q_0\ , \qquad (2.25)$$

where d**A** is the normal vector of the surface of the cubic element. The surface integral can now be calculated for all six sides of the cubical volume element separately, whereas the grad operator in the first term in [Eq.(2.25)] is substituted by its finite difference form

$$\iint \varepsilon(r)\nabla\phi\cdot\mathrm{d}\mathbf{A} = \sum_{i=1}^{6}\varepsilon_i(\phi_i - \phi_0)h\,, \qquad (2.26)$$

where ϕ_0 is the electrostatic potential at the center grid point, ϕ_i is the electrostatic potential at the six neighboring grid points and ε_i is the dielectric constant associated with the center of the line joining the center grid point with its neighbors (see Figure 6). Thus one becomes

$$\sum_{i=1}^{6} \varepsilon_i (\phi_i - \phi_0) h - \bar{k}_0^2 \phi_0 h^3 = -4\pi q_0 , \tag{2.27}$$

Rearranging the equation (2.27) and solving it for ϕ_0 gives

$$\phi_0 = \frac{\sum_{i=1}^{6} \varepsilon_i \phi_i + \frac{4\pi q_0}{h}}{\sum_{i=1}^{6} \varepsilon_i + \bar{k}^2 h^2} . \tag{2.28}$$

The solution of the equation (2.28) is starting from the initial guess for the ϕ at all grid points. Then the new estimates are calculated using equation (2.28). This procedure is repeated until the convergence criterion is met.

Focussing. By using the grid method one should account for a problem, which appears on the boarders of a grid, namely the grid points at the boarders have less than 6 neighbors. This leads to the problem to assign ϕ values for the grid points on the edges. To solve this problem it helps to take a grid, which is much larger than the molecule itself. In this case the points at the outer boundary of cubic grid have vanishing ϕ values, or are calculated from the Debye-Hückel approximation[35]

$$\phi_i = \sum \frac{q_j e^{-kr_{ij}}}{\varepsilon r_{ij}} , \tag{2.29}$$

where r_{ij} is the distance of the j-th charge from the i-th grid boundary point. This expression is a better approximation to the correct values of the electrostatic potential at the boundary than zero. However for a large enough grids, there is no significant difference between setting electrostatic potentials at the boundary of the volume to zero or to the screened coulomb potential from the equation (2.29)[34].

Despite of advantage of using large grids, one is forced to use for larger grid boxes poorer resolution, due to the computer limitations in CPU time and memory. Nevertheless, it is possible to solve this problem by using of the so called “focusing procedure”[55]. An initial calculation is performed on a large grid of lower resolution (Figure 7). This is followed by a computation on a smaller grid with higher resolution,

centered on the region of interest (focusing). The electrostatic potentials on the boundaries of the smaller grid are taken from the interpolated values of the larger grid.

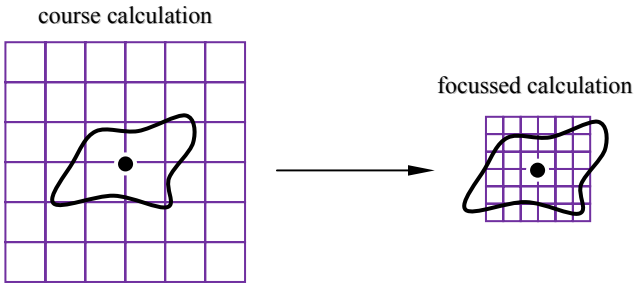

Figure 7. Two-dimensional representation of the focusing procedure.

Grid energy. In the electrostatic computations one is confronted with a problem associated with the self-energy, which is the electrostatic energy of the point charge in its own electrostatic potential, which formally diverges. Usage of discretization on a grid allows to avoid these singularities, since the point charges here are smeared over the grid points in the volume elements. However the self-energy remains in form of so called "grid energy", which is finite, but of an unknown arbitrary value, depending on the grid resolution and position (grid artifact). Nevertheless, it is possible to get rid of the grid energy as follows. Instead of calculation of absolute electrostatic energy one can calculate the energy differences between the systems with the same grid energy (charges and grid resolution and position are unchanged), leading to cancelling of the grid energy.

2.1.2 Continuum electrostatics

2.1.2.1 Dielectric screening

In classical electrostatic theory, materials are considered to be homogeneous dielectric media, which can be polarized by electrical charges. So the solvent molecules and ions in the electric field, generated by the charges of the solute, develop a nonzero dipole moment, or increase it further, if they already possess one. The field created by these induced dipoles is directed against the inducing field, leading to its weakening. This field is called "reaction field". The strength of the reaction field is determined by the magnitude of the inducing field. There are two ways how atoms or molecules can develop the dipole moment in the external electric field: "electronic polarization" and "orientational polarization" (also called "nuclear polarization"). Electronic polarization

refers to the distortion of a molecule's electron clouds by an applied field. Orientational polarizability is limited to molecules with a permanent dipole moment and refers to the tendency of the polar molecules to orient in an electric field. Both electronic and orientational polarizations are contributing to the value of a dielectric constant. Another contribution to the dielectric constant is an atomic polarization, which results from intramolecular vibrations and is estimated to have a small contribution (0.05-0.30) to the dielectric constant[56]. Electronic polarization alone leads to dielectric constants of about 1.5-2.5[56]. The orientational polarization leads to much larger dielectric constants (for example 80 in case of water). Accordingly, instead of explicitly accounting for the polarization of each atom, one can use a dielectric constant as a bulk measure of the polarizability of the media. In this case one speaks of a continuum model.

2.1.2.2 Electrostatic energy

An important property, which can be calculated from the electrostatic potential, is the electrostatic energy. In the simplest case of two charges q_i and q_j the electrostatic energy is given by

$$G^{el} = \frac{q_i q_j}{\varepsilon r_{ij}} = q_i \phi_i \ , \tag{2.30}$$

where r_{ij} is a distance between two charges and ϕ_i is the electrostatic potential at atom i due to a charge at atom j. However, this expression (2.30) is valid only for a homogeneous dielectric, and cannot be applied for modeled system, containing a molecule placed in the solvent. In such a continuum electrostatic model, two regions with different dielectric constants are present: the solute with low dielectric constant and an infinite region with the dielectric constant of the solvent. To calculate the electrostatic energy of such heterogeneous system one can use electrostatic potentials calculated from the Poisson-Boltzmann equation (2.23).

The total electrostatic standard (°) free energy (G°) of the solvated molecular system can be divided into a contribution from the Coulombic interaction of the charges with each other, G_C°, a contribution caused by the interaction of the charges with a polarizable solvent (reaction field energy), G_R°, and a contribution caused by the interaction of the charges with the distribution of ions in the solvent, induced by the charges, G_I°. Hence the total electrostatic energy G° will be given as

$$G^\circ = G_C^\circ + G_R^\circ + G_I^\circ \ . \tag{2.31}$$

Alternatively, the total electrostatic energy can also be represented as a sum of two sets of terms

$$G^{\circ} = G^{\circ}_{ij} + G^{\circ}_{ii} . \tag{2.32}$$

The first set G°_{ij} includes all pairwise interaction energies

$$G^{\circ}_{ij} = G^{\circ}_{C,ij} + G^{\circ}_{R,ij} + G^{\circ}_{I,ij} , \tag{2.33}$$

where $G^{\circ}_{C,ij}$ is a coulombic interaction energy between charges of atoms *i* and *j*, $G^{\circ}_{R,ij}$ represents an interaction energy of the charge on atom *i* with the reaction field induced by the charge on atom *j*, $G^{\circ}_{I,ij}$ is the interaction energy of charge at atom *i* with the ionic distribution in the solution induced by charge on atom *j*.
The second set G°_{ii} includes all self-interaction energies

$$G^{\circ}_{ii} = G^{\circ}_{C,ii} + G^{\circ}_{R,ii} + G^{\circ}_{I,ii} . \tag{2.34}$$

The coulombic self-interaction energy term $G^{\circ}_{C,ii}$ in expression (2.34) is the electrostatic energy of the charge in its own electrostatic potential. As it was already mentioned in the paragraph (2.1.1.2), the self-interaction energy $G^{\circ}_{C,ii}$ is infinite. Nevertheless it can be transformed into finite grid energy by using a grid mapping in the numerical calculations (see paragraph 2.1.1.2). In analytical calculations, the problem of infinite self-energies is avoided by treating charged atoms as spherical shells of uniformly distributed charge[36]. The self-energy thus becomes finite.
The second term in the equation (2.34), $G^{\circ}_{R,ii}$ is an interaction energy of the charge on atom *i* with its self reaction field, and the third term, $G^{\circ}_{I,ii}$ stands for the interaction energy of the charge at atom *i* with the ionic distribution induced by the same charge in the solution.

Using electrostatic potentials calculated from Poisson-Boltzmann equation (2.23) numerically on a grid, one obtains the total electrostatic energy, which includes however the grid energy. Considering a special technique, described above in the paragraph (2.1.1.2), one can get rid of the grid energy by using differences of electrostatic energies.
In such a way it is possible to calculate separate contributions to the total electrostatic energy. In Figure 8 the thermodynamic steps of such procedure are represented. The contribution of G°_{I} can be determined, by performing two finite-difference calculations (see step 3 on the Figure 8). While in both calculations the charges and dielectric

constants are the same, ionic strength in one of them is set to zero, leading to vanishing of G_I° [Eq. (2.31)]. In the difference coulombic and reaction field terms cancel, since

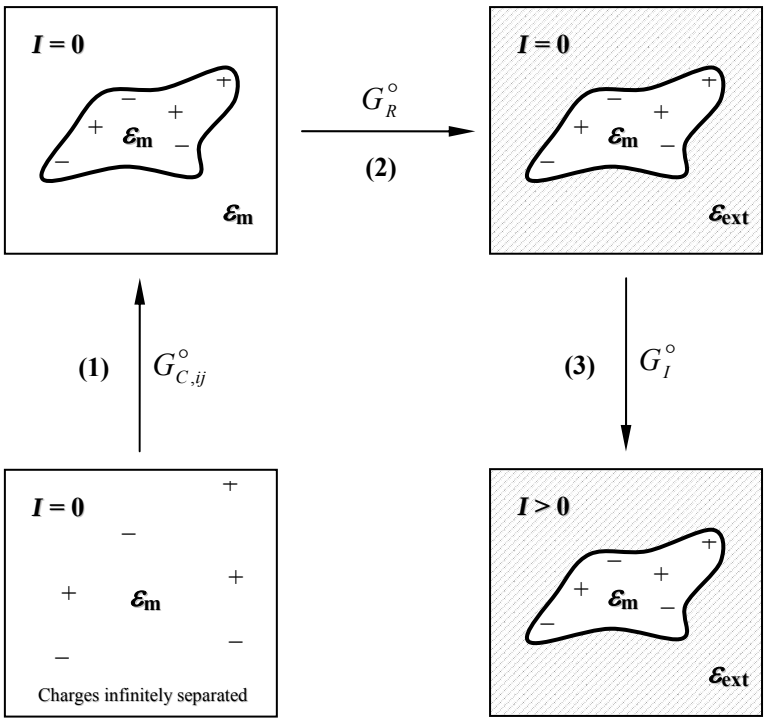

Figure 8. Thermodynamic process for calculation of the contributions $G_{C,ij}^\circ$, G_R° and G_I° to the total electrostatic energy G° of the solute placed in a continuum dielectric. The dielectric constants of the solute and external medium are signed as ε_m and ε_{ext}, respectively. In step 1, the value of the dielectric constant of the external medium ε_{ext} is equal to that of the solute ε_m.

they are in both cases the same. Thus, one obtains

$$G_I^\circ = G^{\circ,(I>0)} - G^{\circ,(I=0)}. \tag{2.35}$$

Similarly, the reaction field term G_R° can be evaluated (step 2 in Figure 8) as a difference of the total electrostatic energies of the system by transferring the solute from the medium having the same dielectric constant as the solute (ε_m) to the medium with dielectric constant of the solvent (ε_{ext}).

The ionic strengths and charges should be kept unchanged. Here the G_C° and G_I° terms [Eq. (2.31)] are canceling in the difference, so that

$$G_R^\circ = G^{\circ,(\varepsilon_{ext};\varepsilon_m)} - G^{\circ,(\varepsilon_m;\varepsilon_m)} \ . \tag{2.36}$$

The first step described in the Figure 8 is a molecular assembly of all charges in a homogeneous dielectric medium with dielectric constant ε_m. The energy of such an assembly, corresponding to the coulombic term $G_{C,ij}^\circ$, is calculated by using Coulomb's law and carried out analytically

$$G_{C,ij}^\circ = \frac{1}{2}\sum_i \sum_{j \neq i} \frac{q_i q_j}{\varepsilon_m r_{ij}} \ . \tag{2.37}$$

The analytical solution of (2.37) doesn't contain self-energy interaction. Adding the terms $G_{C,ij}^\circ$, G_R° and G_I° together yields the total electrostatic energy G_{tot}°, which is free of the grid energy.

2.1.2.3 Solvation energy

Solvation free energy is defined as transfer energy of the ion or molecule from the vacuum into the solvent. Electrostatic solvation energy (ΔG_{sol}°) can be computed as a difference of electrostatic energies [Eq. (2.31)] of the system in solution (ε_{ext}) and vacuum ($\varepsilon_{ext} = 1$)

$$\Delta G_{sol}^\circ = G^{\circ,(\varepsilon_{ext};\varepsilon_m)} - G^{\circ,(1;\varepsilon_m)} \ . \tag{2.38}$$

The electrostatic solvation energy is equal to the reaction field energy of the system, if the inter-atomic space in the solute is "filled" with vacuum ($\varepsilon_m = 1$)

$$\Delta G_{sol}^\circ = G_R^\circ = G^{\circ,(\varepsilon_{ext};1)} - G^{\circ,(1;1)} \ . \tag{2.39}$$

So far only the electrostatic part (ΔG_{sol}°) of the total solvation energy ($\Delta G_{sol}^{\circ,total}$) has been discussed. However additional factors are contributing to the overall solvation energy. Mostly, $\Delta G_{sol}^{\circ,total}$ is considered to have three components

$$\Delta G_{sol}^{\circ,total} = \Delta G_{sol}^\circ + \Delta G_{vdW}^\circ + \Delta G_{cav}^\circ \ , \tag{2.40}$$

where ΔG_{vdW}° is the energy of van der Waals (vdW) interactions between solvent and solute molecules; ΔG_{cav}° is the cavitation energy to form a hole in the solvent, which is ready to insert a solute molecule. The cavitation energy comprises the change in entropy caused by reorganization of the solvent molecules around the solute, and is positive.

The reorganization process mostly affects the solvent molecules in the first solvation shell. Therefore, the entropy costs for reorganization will depend on the number of the solvent molecules in the first solvation shell. This number is approximately proportional to the solvent accessible surface area of the solute (a definition of the solvent accessible surface area is given in the paragraph 2.1.2.4).

Since the van der Waals interaction energy decreases quickly with distance ($1/r^6$), it is also expected to be dependent on the number of the solvent molecules in the first solvation shell of the solute. Therefore it is also roughly proportional to the solvent accessible surface area. Thus the contribution of both van der Waals and cavitation energies can be approximated by following linear expression

$$\Delta G^{\circ}_{vdW} + \Delta G^{\circ}_{cav} = \alpha + \beta S \,, \tag{2.41}$$

where S is the total solvent accessible surface area, and α and β are constants. The coefficients α and β can be taken from the experimentally determined solvation free energies of alkanes. The solvent accessible surface area S can be calculated using, for example the algorithm developed by Shrake and Rupley[57]. Since the van der Waals interaction energy is negative, it is partially compensating the positive cavitation energy.

The contributions from the van der Waals and cavity terms can become significant especially for the uncharged and non-polar solutes. Since the model systems considered in this doctoral work are polar and predominantly charged, the influence of the nonpolar terms (ΔG°_{vdW}, ΔG°_{cav}) relative to the polar term ΔG°_{sol} is generally small and can be neglected.

2.1.2.4 Molecular surface

In continuum electrostatics an important point is the definition of the solute surface. The simplest space-filling representation of the molecular systems is given by merging the atomic spheres defined by de vdW radii of the atoms. It is so-called “van der Waals volume” and the boundaries are the “vdW surface” (Figure 9). However the vdW surface is not suitable for the study of solute-solvent systems, since it does not appropriately describe solvent accessibility. Some of the vdW surface may be buried in the inner regions of the molecule (for example, in proteins), where the solvent has no access (Figure 9). Using an idea of Lee and Richards[58], the outer surface of a protein can be constructed by rolling a solvent-sized probe sphere over the solute molecule (Figure 10). This surface is defined as “molecular surface”.

In 1978 Richmond and Richards have introduced the concept of contact surface[59]. The contact surface is that part of the vdW surface which is in contact with a solvent probe sphere (Figure 11). Soon afterwards, Richards introduced the reentrant surface[60], which is the inward facing part of the probe sphere by contacting more than one atom (Figure 11). The contact surface together with the reentrant surface forms the molecular surface.

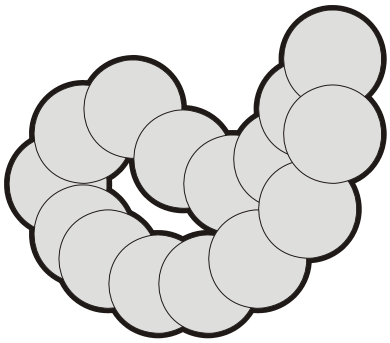

Figure 9. Representation of the van der Waals surface (thick line)

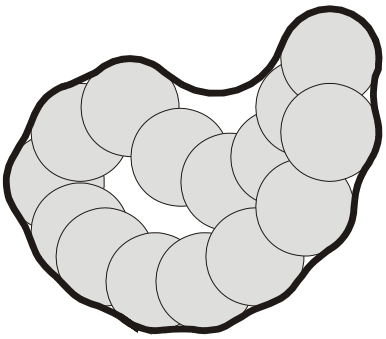

Figure 10. Representation of the molecular surface (thick line)

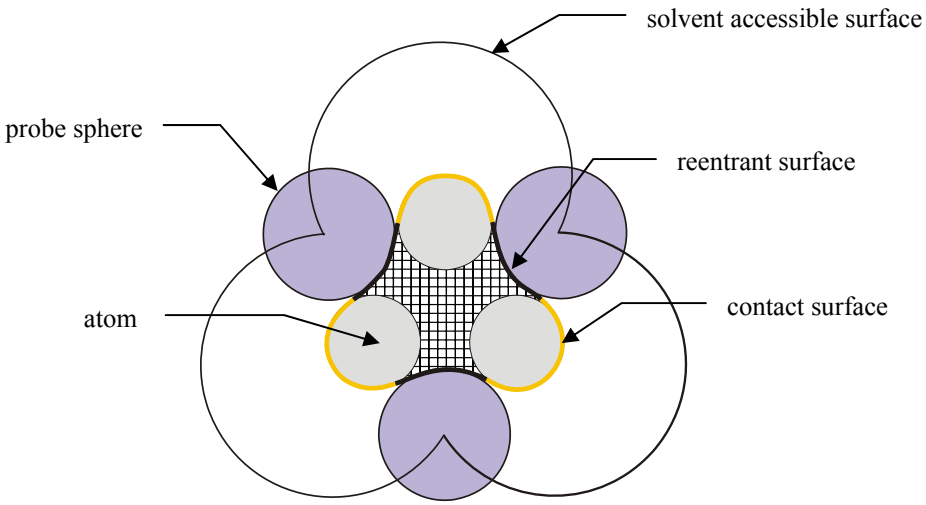

Figure 11. Two-dimensional model describing the surfaces of the solvent molecule. Thick line shows the reentrant (black) and contact (orange) areas, which together form the molecular surface.

The volume captured by the molecular surface was called by M. Connolly "solvent-excluded volume"[61].

Another surface type, relevant for the solute-solvent systems, was introduced by Lee and Richards[58] and called "solvent accessible surface". The solvent accessible surface is traced out by the probe sphere center as it rolls over the molecule of interest (Figure 11). It can be also defined as an expanded vdW surface, which is created by union of the atomic spheres with vdW radii increased by the probe radius (expanded vdW radii).

Nowadays there are number of methods available for the calculation of the solvent-accessible and molecular surface areas. Most popular of them are the algorithms developed by Shrake and Rupley[57], Richmond[62], and Connolly[63, 64]. The topology of the surfaces generated by these methods depends on such factors as vdW radii of the solute molecule and probe radius of the solvent.

In this work program MEAD[53, 54], is used to solve the Poisson-Boltzmann equation, where the boundary between the solute and dielectric continuum corresponds to the molecular surface.

2.1.3 Atomic partial charges

One of the essential parameters in electrostatic energy computations are the atomic partial charges. The atomic partial charges are formed due to the asymmetric distribution of electrons within the molecule. Unfortunately, partial charges are not directly measurable physical quantities, but they can be estimated from the quantum-chemical computations or other molecular properties, which directly or indirectly are related to the electron density distribution in a molecule. Since these methods consider different models and concepts, the determined atomic partial charges depend on the method used for there estimation. In the meantime a number of such methods[65-71] are available, which can be divided in following groups:

charges derived from

1. population analysis of wave functions
2. partitioning of electron density distribution
3. electron density-dependent properties
4. spectroscopic data
5. other experimental data
6. electrostatic potentials (ESP)

Among the listed methods most popular at present is the derivation of the atomic partial charges by the fitting them to reproduce the electrostatic potential, calculated at a large number of grid points around the molecule, using the least-squares procedure. The first important contributions to this area have been done by Momany[72], Scrocco and Tomasi[73], Smit, Derrison, and van Duijneveldt[74], and Cox and Williams[75]. The major advantage of the electrostatic potential derived charges is due to the fact that they optimally reproduce the intermolecular interaction properties of molecules[65]. It presumes however an appropriate level of accuracy of the quantum chemical calculations used for the derivation of the electrostatic potentials at grid points around the molecule of interest. The dependency of ab-initio derived charges from the basis set diminishes significantly by using of the basis set 6-31G* or a larger basis set[65].

2.1.3.1 Charge derivation from electrostatic potential

Unlike the atomic partial charges, the molecular electrostatic potential $\phi(\mathbf{r})$ is in principle an observable quantity and can be determined for each space point from the calculated wavefunction, using equations (2.42) and (2.43)

$$\phi_{\text{nucl}}(\mathbf{r}) = \sum_{A=1}^{M} \frac{Z_A}{|\mathbf{r} - \mathbf{R}_A|}, \tag{2.42}$$

$$\phi_{\text{elec}}(\mathbf{r}) = -\int \frac{d\mathbf{r}' \rho_{\text{elec}}(\mathbf{r})}{|\mathbf{r}' - \mathbf{r}|}, \tag{2.43}$$

$$\phi(\mathbf{r}) = \phi_{\text{nucl}}(\mathbf{r}) + \phi_{\text{elec}}(\mathbf{r}), \tag{2.44}$$

where $\phi_{\text{nucl}}(\mathbf{r})$ and $\phi_{\text{elec}}(\mathbf{r})$ are the electrostatic potentials due to the nuclei and electrons, respectively, Z_A – nuclear charge, $\rho_{\text{elec}}(\mathbf{r})$ - electron density. The least-squares fitting procedure is then used to derive a set of atomic partial charges, that will best reproduce the electrostatic potential at a number of points surrounding the molecule. Equation (2.45) represents the function χ^2_{esp}, which should be minimized during the least-squares procedure

$$\chi^2_{\text{esp}} = \sum_{i=1}^{N} w_i (\phi_i^0 - \phi_i^{\text{calc}})^2, \tag{2.45}$$

where ϕ_i^0 is the electrostatic potential at *i*-th grid point, ϕ_i^{calc} is the electrostatic potential derived from the charge model, *N* is the number of grid points and w_i the statistical weighting factor for the *i*-th point. Since the sum of the charges must be equal

to the total charge of the molecule (Z), each *N*-th partial charge q_N will depend on the values of the others (q_j) as follows

$$q_N = \mathrm{Z} - \sum_{j=1}^{N-1} q_j \,. \tag{2.46}$$

Now the electrostatic potential ϕ_i^{calc} at grid point *i*, which is due to all charges q_j, can be calculated using

$$\phi_i^{calc} = \sum_{j=1}^{N-1} \frac{q_j}{\left|\mathbf{r}_i - \mathbf{r}_j\right|} + \frac{\mathrm{Z} - \sum_{j=1}^{N-1} q_j}{\left|\mathbf{r}_i - \mathbf{r}_N\right|} \,. \tag{2.47}$$

Inserting expression (2.47) in equation (2.45) yields

$$\chi^2_{\mathrm{esp}} = \sum_{i=1}^{N} w_i \left(\phi_i^0 - \sum_{\mathrm{j}=1}^{\mathrm{N}-1} \frac{\mathrm{q_j}}{\left|\mathbf{r}_\mathrm{i} - \mathbf{r}_\mathrm{j}\right|} + \frac{\mathrm{Z} - \sum_{\mathrm{j}=1}^{\mathrm{N}-1} \mathrm{q_j}}{\left|\mathbf{r}_\mathrm{i} - \mathbf{r}_\mathrm{N}\right|} \right)^2 . \tag{2.48}$$

To find the minimum of χ^2_{esp}, the first partial derivatives of χ^2_{esp} with respect to each of the (*N*-1) atomic partial charges must be set to zero resulting linear equations with the atomic charges as unknown. The details of this procedure can be found elsewhere[69].

There are several examples of methods using electrostatic potentials to compute atomic charges, such as CHELP[70], CHELPG[67], Merz-Kollman procedure[68] and RESP[65]. One of the differences between these methods is the way to select the grid points at which the electrostatic potential is calculated[76]. However in all cases the region where the points are generated is the one beyond the van der Waals radii of the atoms involved – it is necessary to avoid getting to close to the nuclei, where the electrostatic potential is always positive[68, 75]. A comprehensive comparison and evaluation of the mentioned methods can be found in the literature[71, 76].

Despite the superiority of the electrostatic potential based methods to other computational charge derivation methods, they have also some weaknesses. The charges generated using these methods are, for example not easily transferable between common functional groups. Another problem is that they depend on the conformation, leading to a number of artifacts in the conformational energetics[65, 77]. One reason for such a behavior is due to the statistical nature of the fitting procedure, which is relatively insensitive to the charges of buried atoms (e.g. sp^3 carbon). The grid points for the

charge fitting procedure must lie outside the vdW surface of the molecule[68, 75]. It is obvious, that under such conditions the charges of buried atoms will be poorly determined, since the even closest grid points are placed relatively far away from them. In general, the less solvent-exposed an atom is, the less well determined is its charge[65]. Among the approaches deriving ESP charges, the mostly used one is the restrained electrostatic potential (RESP) method[65, 77], where some of the above mentioned flaws of classical methods of generating ESP charges are partially rectified.

The RESP method, which will be described in the following paragraph, was used also in the present work to generate the atomic partial charges.

2.1.3.2 Some details of the RESP method

As it was already mentioned in the previous paragraph, that the restrained electrostatic potential (RESP) method[65, 77] belongs to one of the approaches generating charges from the electrostatic potentials derived from the quantum-chemically computed wavefunction. Unlike other methods, it is using restraints in form of a special penalty function in the charge derivation procedure. Using of these restraints helps to considerably minimize the known problems (see paragraph 2.1.3.1) of the ESP methods at the expense of only minor decrease in the quality of the fit of the resulting electrostatic potential compared to that determined quantum chemically[65].

By introducing of the penalty function χ^2_{rstr} to the charge fitting procedure in the RESP method, an additional term is added to χ^2_{esp} so that an error function is represented as

$$\chi^2 = \chi^2_{\text{esp}} + \chi^2_{\text{rstr}} . \tag{2.49}$$

The introduced penalty function has a hyperbolic form

$$\chi^2_{\text{rstr}} = a\sum_{\text{j}}((q_j^2 + b^2)^{1/2} - b), \tag{2.50}$$

where a is a scale factor defining the asymptotic limits of the strength of the restraint and b determines the "tightness" of the hyperbola around its minimum[65]. The hyperbolic form of the restraint function allows to reduce the overall magnitude of the fitted charges, mostly for the statistically poorly determined charges, without exorbitantly penalizing the larger, but better determined charges.

Another kind of constraint which is possible to apply within the RESP protocol is to enforce a symmetry. This constraint is applicable in the cases where, geometrically non-equivalent atoms become equivalent due to rapid exchange (e.g. hydrogen atoms by

rotation of CH_3 or CH_2 group). However, enforcing symmetry leads to unwanted reduction of the ESP in the regions of the polar atoms. As a solution to this problem the developers of the RESP suggested a two-stage approach[65, 77]. In the first stage the fitting procedure is performed with weak restraints and without enforcing symmetry. In the second stage the fitting is carried out only for those groups, which should be symmetrized.

It has been shown[77], that the atomic charges generated using the RESP approach perform quantitatively very well for both solvation free energies and intramolecular conformational energies.

2.2 Referencing of redox potentials

In this paragraph some points will be addressed, which are related to the reference systems used for the experimental determination of the redox potentials. These considerations are important in context of the present work, which relies on available experimental data of redox potentials. These data must be correctly standardized before they can be utilized.

In the experiment the redox potential is measured relative to a reference electrode. The **standard hydrogen electrode** (SHE) is the reference from which all standard redox potentials are determined and has been assigned an arbitrary half cell potential of 0 V. It is very reproducible, showing differences of only 10 μV between different hydrogen electrodes. A typical design is shown in Figure 12.

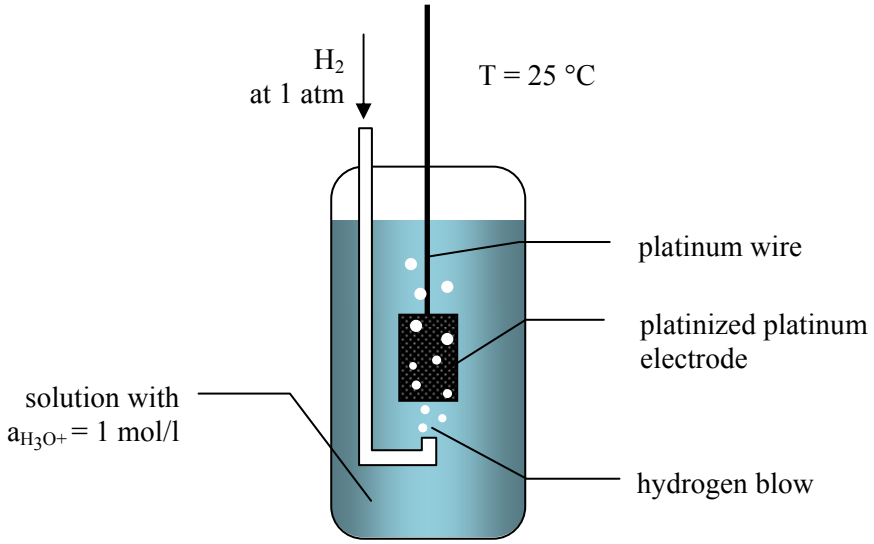

Figure 12. The scheme of the SHE. The platinum foil is suspended in sulfuric acid solution having H^+ unit activity ($a_{H_3O^+} = 1$ mol/l) at 1 atm and 25 °C. In order to maintain $a_{H_3O^+}$ at 1 mol/l, purified H_2 gas is injected into the system. The equilibrium is established between hydrogen and hydroxonium ions in solutions through a platinum electrode coated with platinum black (platinized).

However, in the praxis the experimenters commonly use other reference electrodes, which are more suitable for the studied system. Accordingly, the measured redox potentials are often reported relative different reference electrodes. This complicates the use and comparison of these redox potentials, since the recalculation of their values is needed. The problem is that for some reference systems contradictory redox potential values are reported in the literature[78]. The most critical example is the redox potential of the ferrocenium/ferrocene redox couple (Fc^+/Fc), which is used as an internal

standard. In acetonitrile it appears often to have the value +400 mV versus the SHE[79] and many authors adopt this by recalculation of the data standardized against Fc^+/Fc. They follow obviously the false assumption, that redox potentials are invariant with solvent[79, 80]. This assumption, however has been shown to be incorrect[81]. Other conflicting values (+450 or +400 mV versus SCE) were reported recently[82, 83]. Detailed comparison and critical review of some reference systems was reported by Pavlishuk and Addison[78], which performed direct measurements of these reference electrodes versus each other.

Taking into account the issue addressed above, the author was very careful by the selection of the available experimental redox potentials for the present thesis work. The conversion factors, which were used to transform the redox potentials to the standard hydrogen electrode are following: Ag/AgCl +0.200 V[84], SCE +0.244 V[78], Fc+/Fc in acetonitrile (AN) +0.624 V[78], and Fc+/Fc in dimethylformamide (DMF) +0.702 V[85]. A pictorial representation is given on the Figure 13.

Figure 13. Scale representing the redox potentials of reference electrodes relative SHE

2.2.1 Absolute electrode potential of SHE

In the previous paragraph it has already been mentioned, that half-cell redox potentials are measured relative to the half-cell potential of SHE, which is arbitrarily set to 0. The SHE half-cell reaction is defined as

$$H^+_{water} + e_g \rightarrow \frac{1}{2} H_{2(g)} \ . \qquad (2.51)$$

An important question is to determine the absolute electrode potential of the SHE, defined as a half-cell potential versus a free electron at rest in vacuum[86]. There is substantial interest in this, because the knowledge of this value would allow making comparisons of calculated potentials to measurable values. Considerable effort was applied to answer this question, and numerous estimates have been made for the potential of the SHE versus a free electron[86-93]. Reiss and Heller proposed a value of 4.43 V[88], calculated from the thermodynamic cycle. This cycle includes the work

function of a semiconductor (110 p-InP), the Schottky barrier created between the InP and H_2 saturated Pt, and the potential of zero charge for the Pt surface by contacting water at pH=0. The dipole of InP is assumed in this model to be 0. For the absolute potential of SHE Parsons proposed the value of 4.44 V[89]. He used a thermodynamic cycle, which combines the atomization and ionization energies of hydrogen with the free energy of proton solvation in water. However the values of the proton hydration energy reported in the literature are controversial[94-99]. Recently, Truhlar and Cramer suggested a value of 4.36 V[92], based on the latest gas-phase measurements of proton hydration from Tissandier et al.[98]. The International Union of Pure and Applied Chemistry (IUPAC) recommends the value of 4.44 V, based on the Trasatti's suggestion[86]. Trasatti used an approach, which was similar to Parsons's, but considered slightly different thermodynamic cycle. It includes the potential of zero charge of Hg, with its work function, the potential of an Hg/air/SHE cell, and the contact potential difference between Hg and water. Other values for the SHE absolute potential of 4.73 V and 4.7 V were obtained respectively, by Gomer and Tryson[87]and Hansen and Kolb[90]. However, in a subsequent study, Hansen and co-workers got a different value of 4.456 V[91]. Recently, Donald et al. obtained the absolute potential value of 4.2 V by doing measurements with aqueous nanodrops in the gas phase[93]. Hence there is no general agreement on the absolute value of the SHE potential. The problem is that all these methods include assumptions, and have significant uncertainties.

2.3 Spin states of transition metal complexes

For the description of the bonding nature and electronic structure of coordination compounds two theories are commonly used. These are the **ligand** and **crystal field theories.** In this paragraph only few points from these theories will be shortly touched, which are related to present work.

The electronic structure of an isolated transition metal-ion involves five d-orbitals, which have the same energy (they are degenerated). Coordination of ligands to the metal-ion leads to loss of the degeneracy of the d-orbitals, resulting in their energy splitting. Three-dimensional representations of the five d-orbitals along the x, y, and z axis are given on the Figure 14.

Due to the different orientations of the five d-orbitals in space (Figure 14), they interact differently strong with the electron orbitals of the ligands, which leads to differences in the orbital energy (loss of degeneracy). The character and magnitude of the energy splitting depends on a number of factors. These are:

- ligand strength
- coordination number
- arrangement of the ligands around the metal ion
- nature of the transition metal
- oxidation state of the metal

The orbital energy splitting in the octahedral and tetrahedral ligand field is demonstrated in the Figure 15.

In the octahedral geometry the energy of e_g-orbitals ($d_{x^2-y^2}$ and d_{z^2}) is increasing (Figure 15), since they are directly involved in the repulsive interaction with the orbitals of the ligand. The opposite happens when the four ligands coordinated to metal ion are building a tetrahedral complex: here the t_{2g}-orbitals (d_{xy}, d_{xz}, d_{yz}) are shifted up relative to the e_g orbital (Figure 15). In the ligand field of other possible geometries the d-orbitals show different splitting patterns. Since this energy splittings are not relevant to the current work, they will not be described here in more detail (see more in the literature[40, 41]).

Through the splitting of the d-orbitals both low- and high spin electronic ground states for the transition metal complexes are possible. Such spin states for the related to the current work metal-ions (iron, manganese and nickel) are shown in the Figures 16-18. The factors influencing the orbital energy splitting regulate also the spin states of the

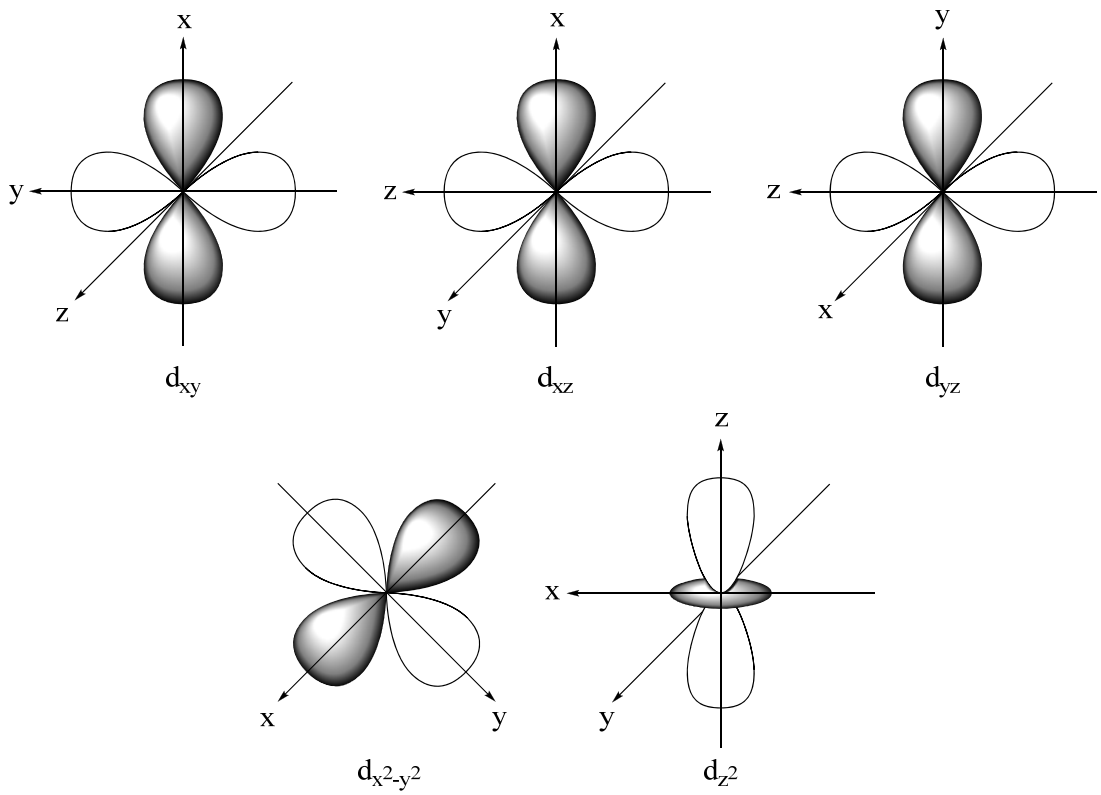

Figure 14. Representation of the d-orbitals along the axis. The colors indicate a phase of wave-function: positive (gray) and negative (white).

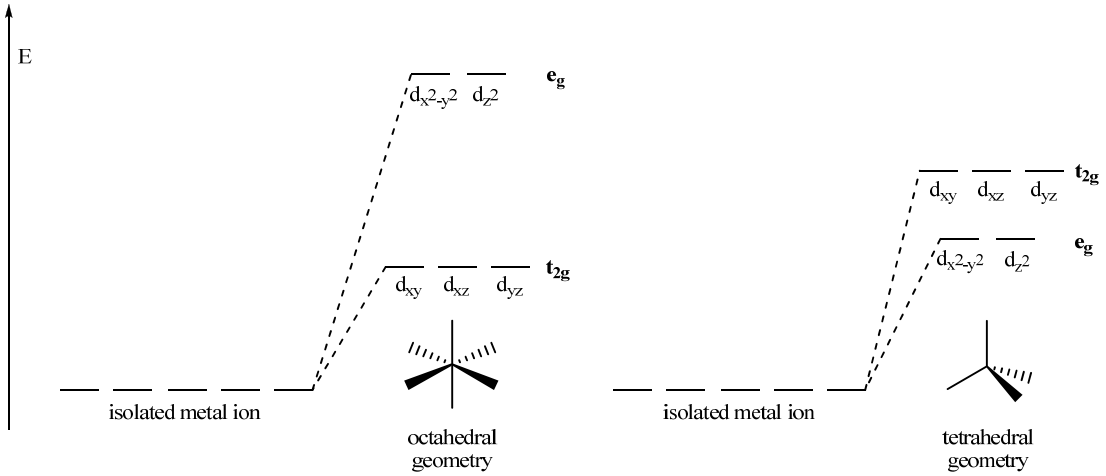

Figure 15. Example of the energy splitting of the d-orbitals in transition metal complexes with identical ligands in octahedral and tetrahedral geometry. Degenerate orbitals remaining after energy splitting are called by convention t_{2g} (d_{xy}, d_{xz}, d_{yz}) and e_g ($d_{x^2-y^2}$, d_{z^2}).

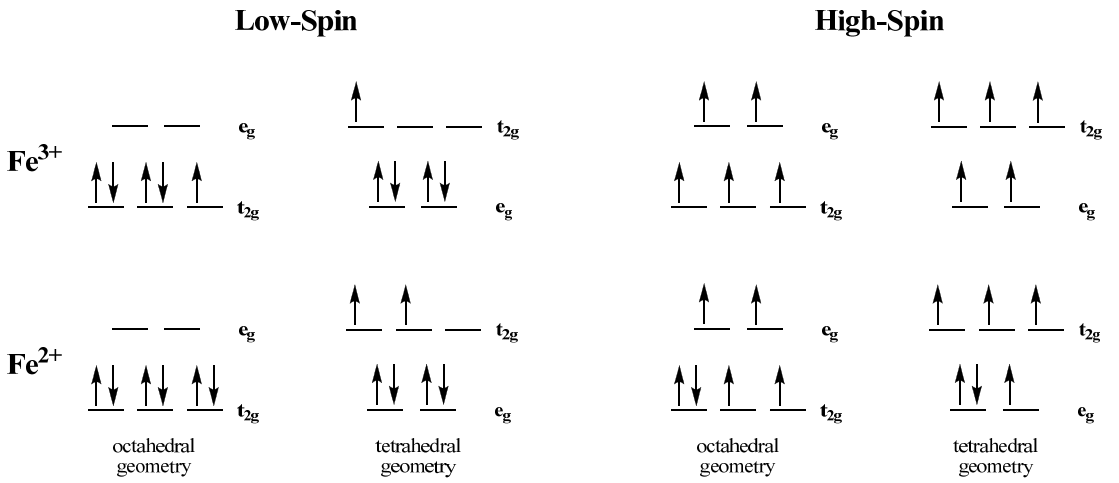

Figure 16. Electronic configuration of Fe^{3+} and Fe^{2+} in the low- and high-spin states for the octahedral and tetrahedral ligand field.

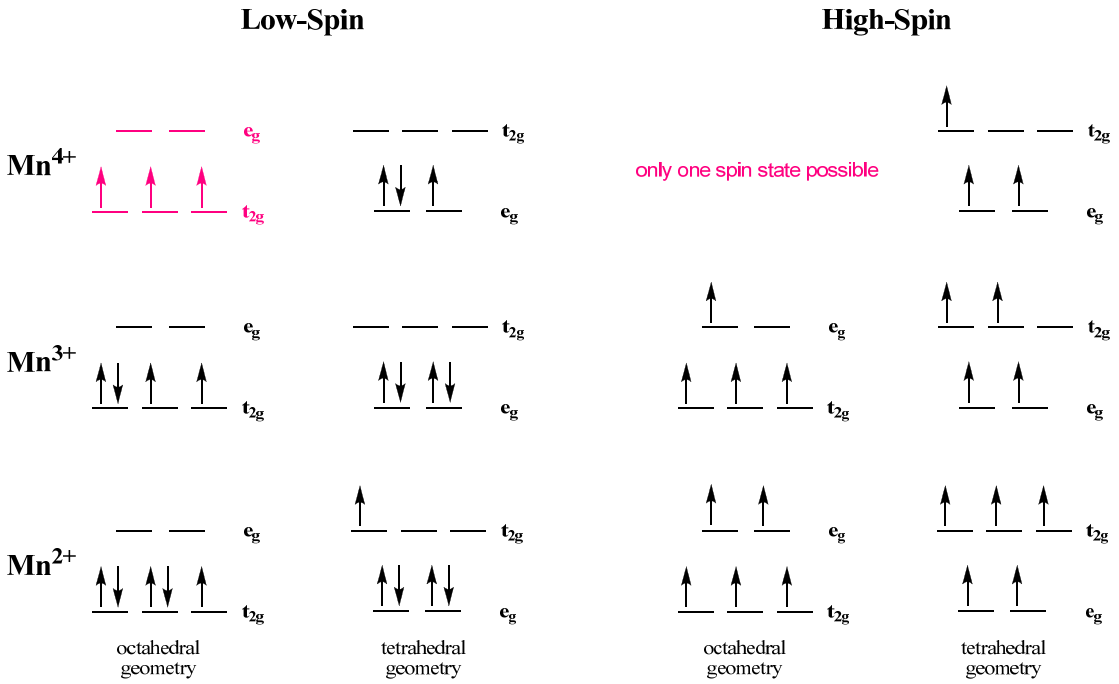

Figure 17. Electronic configuration of Mn^{4+}, $Mn^{3+}$and Mn^{2+} in the low- and high-spin states, for the octahedral and tetrahedral ligand field. The electronic configuration with one possible state (neither low- nor high-spin state) is colored blue.

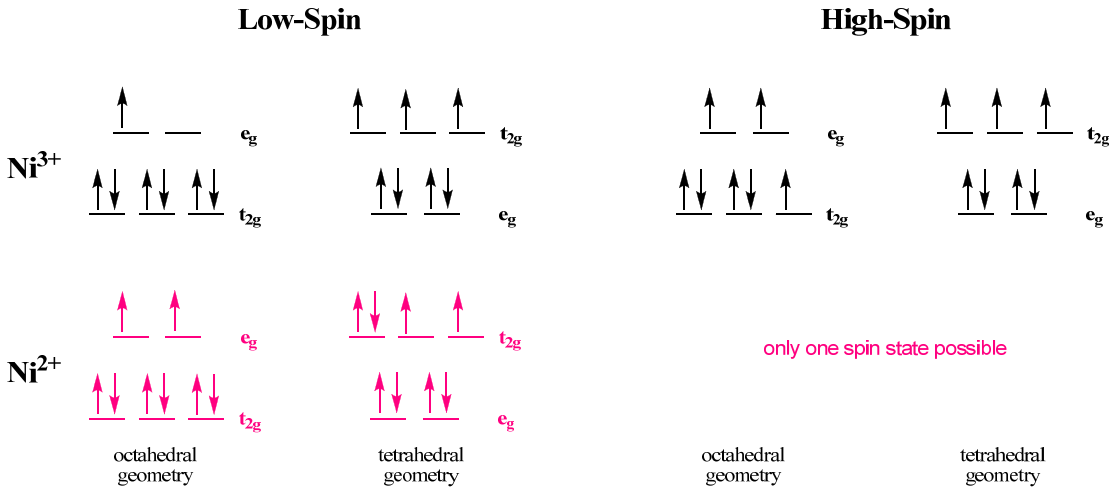

Figure 18. Electronic configuration of $Ni^{3+}$and Ni^{2+} in the low- and high-spin states, for the octahedral and tetrahedral ligand field. The electronic configuration with one possible state (neither low- nor high-spin state) is colored blue.

transition metal complexes. In a weak ligand field the ground state spin multiplicity is maximal (high-spin), whereas strong ligand field stabilizes the low-spin state with minimum spin multiplicity. However, in the ligand fields of intermediate strength the energy difference between the lowest vibronic levels of the potential wells of the two states may be so small, that already minor perturbations are able to effect a change in the state. This phenomenon is called **spin transition** or **spin crossover**. Spin-crossover centers are of great interest, because they are one of the best-known forms of an inorganic electronic switch. Spin crossover effects are known to occur in solid state and in solution. Spin transitions are very important in the biological active systems. The factors which can induce the spin transfer are the thermal energy, pressure and light. Thermally induced spin crossover occurs when the difference between low- and high-spin energy levels of the complex is of about kT. When this criterion is met pressure- or light-induced transitions may also be observed[39].